Copyright © 2014 American Scientific Publishers
All rights reserved
Printed in the United States of America

Journal of
Nanoelectronics and Optoelectronics
Vol. 9, 1–10, 2014

Electrophysical and Photoelectric Properties of Injection Photodiode Based on pSi–nCdS–In Structure and Influence of Ultrasonic Irradiation on them

Sh. A. Mirsagatov[1], I. B. Sapaev[1,*], Sh. R. Valieva[1], and D. Babajanov[2]

[1] Physical Technical Institute, Scientific Production Association "Physics-Sun" Academy of Sciences of Uzbekistan
[2] Turin Polytechnic University in Tashkent, 100095, Tashkent, Uzbekistan

It is shown that in pSi–nCdS–In-structure there is a mutual compensation of drift and diffusive counter-flows of charge carriers. The drift and diffusive counter-flows of non-equilibrium minority carriers at current density of I $\sim(10^{-8}\text{-}10^{-7})$ A/cm^2 lead to occurrence of inversion points of photo-sensitivity sign in shortwave and in longwave spectrum ranges. The mutual compensation of drift and diffusive counter-flows at current density of $\sim 10^{-6}$ A/cm^2 leads to occurrence of a sub-linear region on reverse current–voltage characteristic in a wide range of bias voltage. It is established that pSi–nCdS-heterojunction has rather low density of surface states, that allows on a basis of pSi–nCdS–In-structure to obtain an injection photo-detector with high spectral ($S_\lambda = 5.04 \cdot 10^4$ A/W) and integrated ($S_{\text{int}} = 2.8 \cdot 10^4$ A/lm or $4.47 \cdot 10^6$ A/W) sensitivity in a direct current direction. It is established that ultrasonic processing of such photo diodes leads to reduction of density of surface states on heterojunction interface and raises the spectral and integral sensitivity of photodiodes and that is clarified by ultrasonic annealing of defects on interface.

Keywords: Injection, Heterostructure, Spectrum, Photosensitivity, Ultrasonic Annealing.

RESEARCH ARTICLE

1. INTRODUCTION

There are well known data on formation of injection photodiodes based on A^2B^6 connections, in particular based on sulfide and cadmium telluride and its solid solutions.[1–4] The Ni–nCdS–n$^+$CdS-structure based on CdS mono-crystals is considered to have photocurrent strengthening when it is illuminated with $\lambda = 0.22$ microns light since there is an injection of the majority charge carriers in a high-resistance n-area from non-illuminated side of n^+-n-transition.[1] The injection photo-detector with internal strengthening based on the cadmium sulfide, working at room temperature in a wide range of spectrum is not created yet. Such injection photo-detector with increased output parameters can be created on the p–i–n-based structures. For A^2B^6 semiconductors, including CdS, it is technologically difficult to obtain p-type conductivity and p–i–n-structure on its basis because of self-compensation effect. To avoid this problem we created pSi–nCdS–In-structure with heterojunction. The high-resistant strongly compensated weak n-type CdS-layer plays role of i-layer here. The choice of pSi–nCdS heterojunction was previously described.[5] On the other hand, silicon is a well studied material. Weak side of such structure is pSi–nCdS heterojunction, because of lattice constants and thermal expansion coefficients of cadmium sulfide and silicon differ essentially, therefore the density of edge states on heterojunction interface can be considerable. To decrease density of edge states the structure was subjected to ultrasonic annealing.

The fact that the ultrasonic irradiation (USI) influences the defective structure and an electro-physical characteristic of semiconductors and semi-conductor structures is well established.[6–11] To advantages of USI in comparison with thermal annealing and radioactive irradiation it is possible to refer to the following features: (1) absorption of ultrasonic waves in a solid body occurs mainly in periodicity breaking areas of its crystal lattice and consequently ultrasonic influence has more local character; (2) using ultrasonic waves of various polarization and type allows to raise the selectivity of their influence; (3) by tuning the frequency of ultrasonic fluctuations it is possible to reach resonance transformations in a defective subsystem.

The aim of this work is to establish the ultrasonic irradiation influence on electrophysical and photoelectric properties of the injection photodiode based on pSi–nCdS–In structure.

*Author to whom correspondence should be addressed.

2. SAMPLES AND A MEASUREMENT TECHNIQUE

The photosensitive pSi–nCdS–M-structure has been created by deposition of CdS layer under 10^{-5} torr vacuum on a surface of *p*-type silicon plate with specific resistance $\rho \approx 10\ \Omega \cdot$cm and thickness 300$\mu$m.[12] Thus, the CdS source temperature T_{source} was maintained at 800–850 °C and a substrate (pSi) $T_{substr} = 250$–300 °C. Observation under the microscope MII-4 have shown that CdS films grown on pSi-substrate consist of columnar crystallites which are oriented in a direction of films growth and disorientated on an azimuth direction. We established that the crystallite size depends strongly on technological modes and first of all on temperature of Si-substrate. For example, CdS films which have been made at $T_{substr} = 300$ °C, have the crystallites size of 3–4 μm which completely penetrated through films thickness of $w \approx 2$ μm. Obtained CdS films were high-resistive, with specific resistance $\rho = 2$–$3 \cdot 10^{10} \Omega \cdot$cm and weak *n*-type conductivity. Further, the barrier has been obtained by sputtering of indium on a surface of CdS film in 10^{-5} torr vacuum during 25–30 s at substrate temperature 373 K.

The current-collecting "Π"-shaped contact also was formed by vacuum evaporation of indium.

Current–voltage characteristics (*C–V* characteristics) of pSi–nCdS–In structures were measured in a direct and inverse current directions, first in dark and then on light, at $E = 0.1 - 100$ lux and room temperature. Illumination of structures was made by LG-75 laser with radiation power of 0.01–0.75 mW/cm^2 and wave length of 0.625 μm and also by an incandescent DKSSH-1000 type xenon lamp with radiation power in one lumen in visible area of a spectrum is $9.1 \cdot 10^{-3}$ W.[13] The spectrum dependence of structure photosensitivity was measured on ZMR-3 monochromator at 300 K. The DKSSH-1000 xenon lamp working in a mode of minimum power-carrying power provided a light flux of 53000 lm and brightness up to 120 MCd/m^2 in the center of a light spot. The lamp radiation was calibrated in absolute units by means of thermosensor RTE-9 with a quartz window. The DKSSH-1000 lamp has a continuous spectrum in ultra-violet and visible regions.

The ultrasonic irradiation (USI) was carried out with 1 W power, frequency of a test signal $f = 2.5$ MHz during 15 min.

3. EXPERIMENTAL RESULTS AND DISCUSSION

In Figure 1 the direct and inverse branches of *C–V* characteristics of typical pSi–nCdS–In structure are presented in half-logarithmic scale. "+" potential applied to pSi contact considered as forward direction of a current in structure and with "−" potential-as backward. *C–V* characteristics analysis shows that the structure has rectification properties and its rectification factor "*K*" (defined as the ratio of a direct and inverse current at fixed voltage $U = \pm 20$ V) is $\approx 10^5$.

4. SPECTRAL DISTRIBUTION OF PHOTOSENSITIVITY

The curve analysis of spectral distribution of photosensitivity S_λ in a direct current shows (Fig. 2(a)) that it has a spectral range $\lambda = 389 - 1238$ nm. The spectral sensitivity of such structure begins with $\lambda = 389$ nm and grows promptly, reaching the maximum at $\lambda = 480$ nm, where $S_\lambda = 2.7$ A/W. Then the spectral sensitivity decreases to zero at $\lambda = 872.7$ nm. On a curve of decreasing photosensitivity there is a number of features shown in the form of step at $\lambda = 541.8 - 578.6$ nm and three small peaks at $\lambda = 618$ nm, $\lambda = 740$ nm and $\lambda = 821.8$ nm. These features are likely to be caused by presence of impurity in cadmium sulfide layers.

Further, after zero value of spectral sensitivity at $\lambda = 872.7$ nm, it changes the sign, begins to grow and at $\lambda = 961.8$ nm the maximum point with $S_\lambda \sim 0.2$ A/W is observed. Then there is its smooth decay with increase S_λ value to zero ($\lambda = 1042.8$ nm) and then again there is its growth (with sign change) and at $\lambda = 1200.3$ nm it reaches a maximum where $S_\lambda \sim 0.93$ A/W. Then with increase in wavelength the value of spectral sensitivity starts to fall.

Under superposition of bias voltage the form of dependence S_λ (λ) does not change and only increases the magnitude of spectral sensitivity, especially, at $\lambda_1 = 480$ nm and $\lambda_2 = 872.7$ nm, where S_λ peaks are observed. For example, $S_\lambda = 2.7$ A/W at $U = 0$ V and $S_\lambda = 4.1$ A/W at $U = 2$ mV. The similar picture can be observed for the second peak ($\lambda = 961.8$ nm), where $S_\lambda = 0.9$ A/W at $U = 0$ V and $S_\lambda = 1.37$ A/W at $U = 2$ mV. This data show that In–nCdS barrier and pSi–nCdS heterojunction effectively divide the generated electron–hole pairs and there is an internal amplification in structure. Thus on an overwhelming part of a spectral range of photosensitivity, S_λ is much larger than spectral sensitivity of an ideal photo-detector (Fig. 2(a), curve 4). An ideal photo-detector is such photo-detector at which all falling photons are absorbed and generate electron–hole pairs, which divided by a potential barrier without lost and give the contribution to a photocurrent. The experimental value of spectral sensitivity in a wide range of a spectrum considerably exceeds S_λ values of ideal photo-detector that indicates the presence of internal amplification. That is why the investigated structure is very sensitive to small light levels. The high value of integral and spectral sensitivity is observed both in intrinsic and in impurity areas of light absorption.

Spectral sensitivity in the opposite current direction in absence and in the presence of bias voltage of various magnitudes is shown on Figure 2(b). Apparently from the Figure 2(b), curve 1, in the absence of bias voltage the range of spectral sensitivity lies in the field of wavelengths $\lambda = 350$–1350 nm and has the highest magnitudes

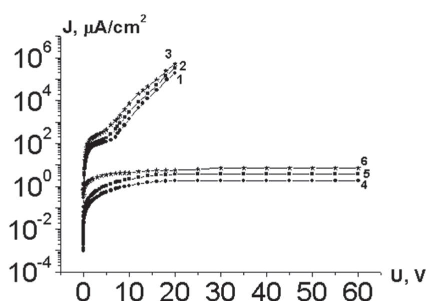

Fig. 1. Current–voltage characteristic of pSi–nCdS–In-structure in half-logarithmic scale in dark and on light before and after ultrasonic irradiation at room temperature: Direct branch before USI (1), direct branch after USI (2), direct branch after USI at light exposure $E = 0, 1$ lux (3), inverse branch before USI (4), inverse branch after USI (5), inverse branch after USI at light exposure $E = 0, 1$ lux (6).

at $\lambda_1 \approx 480$ nm and $\lambda_2 \approx 1248$ nm, where the photocurrents have negative values. From curve 1 of Figure 2(b) one can see that increasing of wavelength of external light spectral photosensitivity reaches zero value at $\lambda \approx 865.45$ nm and further increasing of wavelength leads to the sign change in S_λ (λ) with reaching the maximum value of photosensitivity. In long-wave range the peak appears at $\lambda \approx 949.5$ nm in the field of positive value of a photocurrent. Further, the value of S_λ decreases again and passes through zero at $\lambda \approx 1000$ nm and then photosensitivity, changing a sign, increases sharply on absolute

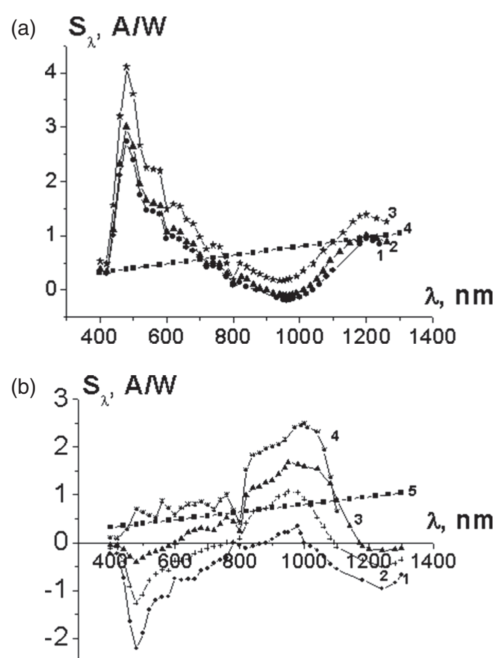

Fig. 2. (a) Spectral dependence of photosensitivity of pSi–nCdS–In structure in the absence and at various bias voltages applied at direct current direction to USI: 1–spectral sensitivity in the absence of bias voltage, 2–0,5 mV, 3–2 mV. (b) Spectral dependence of photosensitivity of pSi–nCdS–In-structure in the absence and presence of various bias voltage at direct current direction to USI: 1–spectral sensitivity in the absence of bias voltage, 2–4 mV, 3–6 mV, 4–8.5 mV.

value to $\lambda \approx 1130$ nm. With the further increase in wavelength it decreases again. At bias voltage giving an inversion point of photocurrent sign in a short-wave area of a spectrum moves strongly aside the shorter wavelengths and the absolute value of a photocurrent decreases with growth of bias voltage magnitude (Fig. 2(b)). The similar behavior of a photocurrent in S_λ (λ) dependence is observed in long-wave area of photosensitivity. However, the inversion point of photocurrent sign moves towards the long waves of electromagnetic radiation. Besides, the speed of change of absolute value of a photocurrent depending on bias voltage is much less, than in short-wave region of a spectrum. For example, the inversion point of photocurrent sign moves on ~260 nm at voltage $U = 6$ mV and in long-wave region of a spectrum it only moves on 168 nm. The experiment shows that at bias voltage 8.5 mV on a structure of the S_λ (λ) dependence completely is in region of positive values of a photocurrent (Fig. 2(b), curve 4). Such behavior of S_λ (λ) dependence of backwards displaced pSi–nCdS–In structure can be explained as follows. First, In–nCdS-transition and pSi–nCdS heterojunction effectively divide non-equilibrium electron–hole pairs generated by light. Second, pSi-nCdS heterojunction injects electrons into the base of (nCdS) structure when bias voltage supplied. Third, the value of bipolar diffusive current increases in the base of investigated structure with increase of backward voltage. Fourth, the barrier of In–CdS is ideal with respect to pSi–nCdS heterojunction.

In pSi–nCdS–In-structure, the electrons are injected from pSi layer into the high-resistance compensated nCdS layer, at sufficient concentration of electrons in pSi layer or if its thickness is comparable with diffusion length of electrons. In a silicon substrate the concentration of equilibrium holes and electrons are equal to correspondingly $1.3 \cdot 10^{15}$ and $7.7 \cdot 10^4$ cm^{-3}, at values of $\mu_n = 1500$ cm^2/V $\cdot$ s and $\mu_p = 480$ cm^2/V $\cdot$ s-electrons and holes mobility, $n_i = 10^{10}$ cm^{-3} concentration of own carriers. Hence, concentration of non-equilibrium electrons in pSi substrate is almost the same as the concentration of electron ($n_o \approx 10^5$ cm^{-3}) in base of (nCdS-layer) which is defined at values: $\rho_{\text{CdS}} \approx 3 \cdot 10^{10}$ $\omega \cdot$ cm and $\mu_n = 100$ cm^2/V $\cdot$ s.[14] Besides, it is necessary to consider the probability of electrons injection from ohmic contact (In) put on pSi, because thickness of a silicon plate is same order with length of diffusion electrons (L_n) which is equal to ≈400 μm at values: $\tau_n \approx 50$ μs and $\mu_n = 1500$ cm^2/V $\cdot$ s.[15]

Peak occurrence on curve photosensitivity with a maximum at $\lambda = 947$ nm allows to assert that the volume charge of pSi–nCdS heterojunction effectively moves the non-equilibrium holes generated in base to pSi-layer. The photocurrent increase in a peak and its expansion towards the short waves with supplied bias voltage shows that the value of bipolar diffusive current of non-equilibrium minority carriers (holes) in the base of structure increases with increase of bias voltage supplied for maintenance of

RESEARCH ARTICLE

an electro-neutrality of injected electrons from pSi–nCdS heterojunction. Due to the high-resistant base of the structure, non-equilibrium carriers are diffused in the form of plasma on the direction, which coincides with a direction of diffusion of minority hole carriers.[16]

Occurrence of inversion point depending on spectral distribution of a photocurrent lets to assert that opposite directed currents in the base of structure compensate completely each other in a certain thickness of base. This thickness of base corresponds to depth of electromagnetic radiation absorption. Shift of inversion point of photosensitivity towards the short waves is defined by value of bipolar diffusion current which is connected with electrons injection from pSi–nCdS heterojunction to the base. This point shifts on small inverse bias voltage. The experiment shows that after giving of bias voltage $U \geq 8.5$ mV the bipolar diffusion current in structure becomes decisive and consequently in a spectrum of photosensitivity distribution photocurrent inversion is not observed.

The analysis of spectral sensitivity of peak of a long-wave range shows that there are electrons injected from ohmic contact (In) in pSi substrate which create diffusion fluxes of electrons and drift fluxes of electrons, directed towards pSi–nCdS heterojunction. Besides, the diffusion fluxes of non-equilibrium electrons, directed from heterojunction to the metal contact appear as a result of electrons accumulation at heterojunction. Shift of inversion point of a photocurrent in long-wave area of a spectrum towards the longer waves shows that diffusion current directed towards to drift and diffusive fluxes of electrons from metal contact, increases with increase in bias voltage.[17,18] It occurs in the case when concentration and a gradient of electrons at heterojunction becomes more than their concentration near to metal contact (In). Such effect takes place, when pSi–nCdS heterojunction possesses a potential barrier and does not let all electrons arriving from the opposite In-contact. Shift of long-wave area of a spectrum at bias voltage $U_{\text{shift}} = 8.5$ mV becomes less, than at $U_{\text{shift}} = 6$ mV. It shows that pSi–nCdS heterojunction becomes throughput for electrons, i.e., the process of electrons accumulation decreases because of change of heterojunction properties.

The analysis of spectral distribution of photosensitivity in the opposite current direction also confirms the above made assumption that from pSi–nCdS heterojunction the electrons are injected to the base.

Ultrasonic irradiation changes spectral dependence of photosensitivity. On Figures 3(a), (b) the spectral dependence of photosensitivity in absence and presence of bias voltage in direct and inverse current directions after ultrasonic irradiation are presented. Apparently from Figure 3(a) the spectral sensitivity in a direct direction of a current after ultrasonic irradiation increases in all spectral range. However, most vividly it is shown in the field of own absorption of cadmium sulfide and silicon. However, at giving of bias voltage the degree of increase in

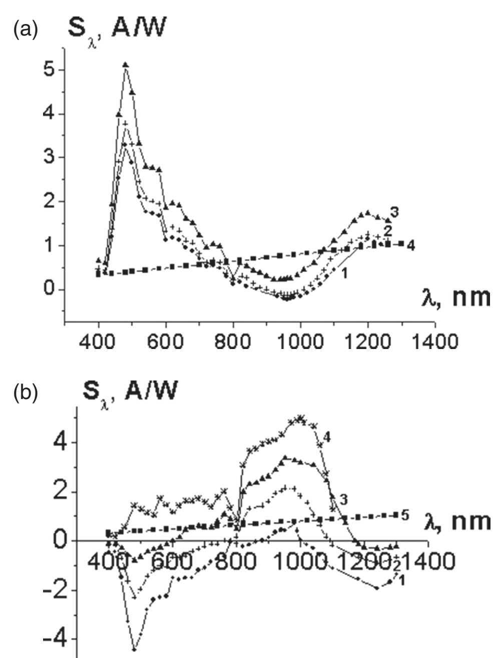

Fig. 3. (a) Spectral dependence of photosensitivity of pSi–nCdS–In-structure in the absence and presence of various bias voltage at direct current direction to USI: 1–spectral sensitivity in the absence of bias voltage, 2–0,5 mV, 3–2 mV. (b) Spectral dependence of photosensitivity of pSi–nCdS–In structure in the absence and presence of various bias voltage at direct current direction to USI: 1–photocurrent in the absence of bias voltage, 2–4 mV, 3–6 mV, 4–8.5 mV.

spectral sensitivity increases. For example, $S_\lambda = 2.7$ A/W at $\lambda = 480$ nm and $U = 0$ V and after ultrasonic irradiation $S_\lambda = 3.2$ A/W at $\lambda = 480$ nm and $U = 0$ V; $S_\lambda = 2.97$ A/W at $\lambda = 480$ nm and $U = 0.5$ mV and after ultrasonic irradiation $S_\lambda = 3.72$ A/W at $\lambda = 480$ nm and $U = 0.5$ mV; $S_\lambda = 4$, 1 A/W at $\lambda = 480$ nm and $U = 2$ mV and after ultrasonic irradiation $S_\lambda = 5$ A/W at $\lambda = 480$ nm and $U = 2$ mV. The similar picture can be observed in the field of own absorption of silicon. For example, $S_\lambda = 0.9$ A/W at $\lambda = 1200$ nm and $U = 0$ V and after ultrasonic irradiation $S_\lambda = 1.1$ A/W at $\lambda = 1200$ nm and $U = 0$ V; $S_\lambda = 1$ A/W at $\lambda = 1200$ nm and $U = 0.5$ mV and after ultrasonic irradiation $S_\lambda = 1.26$ A/W at $\lambda = 1200$ nm and $U = 0.5$ mV; $S_\lambda = 1.37$ A/W at $\lambda = 1200$ nm and $U = 2$ mV and after ultrasonic irradiation $S_\lambda = 1.74$ A/W at $\lambda = 1200$ nm and $U = 2$ mV. The curve 2 (Fig. 3(a)) shows that after ultrasonic irradiation the degree of amplification of a primary photocurrent both in intrinsic and in extrinsic areas of absorption of cadmium sulfide and silicon rises. However, an effect of additional amplification after ultrasonic irradiation is observed more vividly in areas of intrinsic absorption of cadmium sulfide and silicon. It is caused by the big value of a primary photocurrent in these areas of spectrum. Besides, it must be noticed that value of S_λ in the field of intrinsic absorption of cadmium sulfide is much more, than the spectral sensitivity in the field of intrinsic absorption of silicon. It means that on section

border of pSi–nCdS heterojunction the density of edge states is more than at the Schottky barrier of In–nCdS. As it was above specified, the amplification of a primary photocurrent occurs both at intrinsic and at extrinsic areas of cadmium sulfide and silicon absorption, whence follows that in the process of photocurrent amplification participate two mechanisms: positive feedback[19] and the parametrical mechanism.[20,21] In the mechanism of positive feedback the resistance of base is modulated by "intrinsic" light and in the parametrical mechanism the amplification is due to direct modulation of mobility μ under action of extrinsic illumination. As it is specified above, in investigated samples the bipolar diffusion of the current is responsible for amplification of a primary photocurrent. The reason of increase of value of bipolar diffusive current after ultrasonic irradiation in a direct branch of C–V characteristics can be the reduction of density of edge states on the section border of pSi–nCdS heterojunction. So in investigated pSi–nCdS–In-structure in a direct direction of a current the potential barrier formed in a layer of cadmium sulfide created at formation of pSi-nCdS heterojunction is the main obstacle in a way of non-equilibrium electrons, therefore the properties and quality of this heterojunction plays a defining role in charge transfer.

The ultrasonic irradiation distinctly influences the spectral distribution of photosensitivity of pSi–nCdS–In-structure when it is included in the opposite direction of a current. Apparently dependence of S_λ (λ) does not change the form independently on the presence or absence of bias voltage. However after ultrasonic irradiation the injection ability of pSi–nCdS heterojunction increases, that is testified by the increase of bipolar diffusive current value in the base of structure. It is obvious in the area of own absorption of silicon when an inverse bias voltage applied on the structure. The larger the bias voltage, the stronger increase of S_λ (λ) after ultrasonic irradiation. As soon as in this area of a spectrum the direction of a primary photocurrent and an injection current coincide, the process of amplification after ultrasonic irradiation is more pronounced. For example, in the field of waves length (390–1350) nm S_λ $(\lambda) \approx (0.9–2.2)$ A/W before ultrasonic irradiation and after-(1.8–4.5) A/W, hence, it increases approximately twice.

In the field of wave lengths (390–800) nm, the value of S_λ (λ) after ultrasonic irradiation doesn't change much and all depends on what kind of inverse voltage is submitted on structure and, hence, what value has an injection of bipolar diffusive current. In this spectral area a direction of a primary photocurrent and an injection bipolar diffusive current (from pSi–nCdS heterojunction) do not coincide. They are on the opposite direction to each other, therefore the general current in a circuit is equal to a difference of these currents and it changes with difficulty at inverse bias voltage supplied. This phenomenon is more visually shown by comparison of curves of spectral distribution of photosensitivity at lack of external bias voltage before and after ultrasonic irradiation. (Fig. 3(b)). First, after ultrasonic irradiation S_λ decreases in all short-wave range of a spectrum (390–800 nm), especially it is more vivid in the field of own absorption of cadmium sulfide where S_λ decreases from value 4.4 A/W to 2.2 A/W. These experimental results definitely show that directions of primary photocurrent and injection bipolar diffusive current have an opposite orientation and there is an annealing of edge states at ultrasonic irradiation. As a result, the injection ability of pSi–nCdS heterojunction under the influence of photo voltage increases, that promotes increase of injection bipolar diffusive current value in base.

Comparison of S_λ (λ) under various small bias voltages before and after ultrasonic irradiation shows that degree of increase in spectral sensitivity after ultrasonic irradiation becomes more appreciable at giving of bias voltage $U \geq 8.5$ mV. The cause is, that at such value of inverse voltage the share of bipolar diffusive current in the general current becomes defining and consequently the degree of S_λ increase in a range of wavelengths (390–800) nm is more prominent and the photocurrent rise approximately twice after ultrasonic irradiation.

Thus, the analysis of S_λ (λ) of an inverse branch of C–V characteristics before and after ultrasonic irradiation also shows that the increase of the inverse dark and light currents and accordingly the increase of spectral sensitivity is caused by annealing of edge states on N_{ss} border of pSi–nCdS-heterojunction.

For the proof of above made assumption, the density of edge states and its distributions depending on surface potential on border of pSi–nCdS heterojunction before and after ultrasonic irradiation was determined from capacitance–voltage characteristics. Capacitance–voltage characteristic of investigated samples shows the presence of MDP-structure (Fig. 4). It could be explained, since in pSi–nCdS–In-structure the nCdS is the high-resistant and compensated material and, consequently, this layer and oxide layers formed in the process of CdS sputtering on a surface of a silicon plate in vacuum can behave like dielectrics. The density of edge states of MDP-structure is

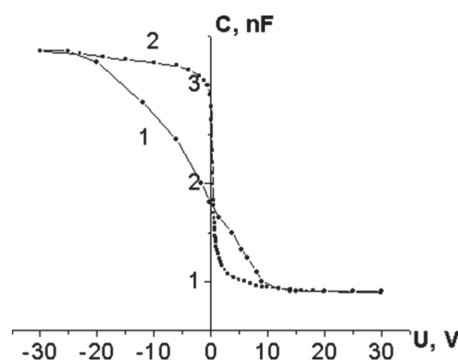

Fig. 4. Capacitance–voltage characteristic of pSi–nCdS–In-structure at frequency of $f = 10$ kHz, $T = 300$ K.

RESEARCH ARTICLE

determined from shift of experimental C(U)-characteristics related to of an theoretical curve at the same value of capacitance:[22] $N_{ss} = \Delta U \cdot C/q$.

On Figure 4 the experimental (1) and expected (2) capacitance–voltage characteristic of a typical injection photo-detector based on pSi–nCdS–In-structure are presented. The expected capacitance–voltage characteristic has been constructed as in. Ref. [22] The experimental capacitance–voltage characteristics has been obtained with a test signal frequency $f = 10$ kHz at room temperature. As at the given frequency the capacitance–voltage characteristic of MDP-structure is clear, the N_{ss} is the slow edge state in heterojunction. For construction of expected capacitance–voltage characteristics the concentration of equilibrium holes carriers in the semiconductor from experimental C(U) of a curve has been determined.[22] The equilibrium concentration of p_0, defined of an abrupt site of C–V-characteristic, constructed in co-ordinates $1/C^2$ (U) and also on capacitance of flat zones[22,23] has appeared to be equal to $\approx 3 \cdot 10^{15}$ cm^{-3} that is, it well conforms with equilibrium concentration of holes in initial p-type silicon.

It is known that the saturation area of C–V-characteristics in MDP-structures based on p-type semiconductors at negative polarity of potential on the top metal electrode (In) is caused by capacitance of dielectric layer. From capacitance it is possible to define a thickness of dielectric layers under the formula of the flat capacitor:

$$d = \varepsilon \cdot S/C_i \qquad (1)$$

where: ε-a dielectric constant, S-the structure area, C_i-capacitance of dielectric layer.

From value of capacitance $C_i = 3.36$ nF at area structure $S \approx 0.1$ cm^2 the thickness of a dielectric layer $d_i \approx 0.06$ μm has been derived. This value differs from a thickness of high-resistance base (nCdS) which is equal to ≈ 2 μm. Such difference could be explained by oxide layers SiO_x, CdO_x and SO_x which thickness is much less than thickness of nCdS.

The value of surface potential (ψ_S) at the set bias voltage (Fig. 5) and dependence N_{SS} from ψ_S (Fig. 6) was defined as described in Ref. [24].

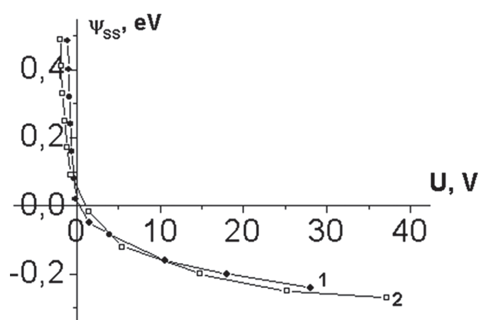

Fig. 5. Dependence of surface potential on the enclosed bias voltage before (1) and after (2) USI.

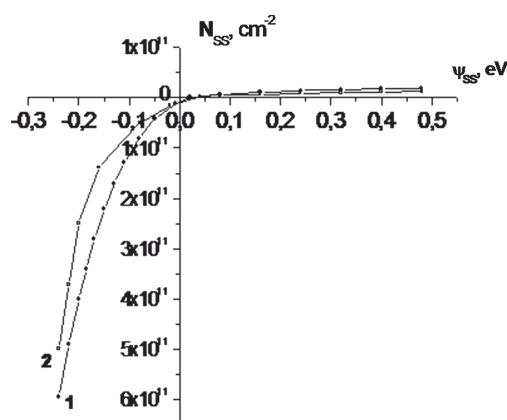

Fig. 6. Dependence of effective density of edge states on surface potential before (1) and after (2) USI.

The analysis of dependence $U(\psi_s)$ shows that at thermodynamic equilibrium the surface potential is $\psi_s = 0.04$ eV. That means domination of negatively charged acceptor edge states on the border which on grasping the holes from a valence band, passes to a neutral condition and bend zones downwards. From the Figure 5 also follows that the condition of flat zones is realized at positive bias voltage giving $U = 1.68$ V on In-electrode then the bend of zones occurs to the further growth of bias voltage upwards. At negative potential on In-layer the investigated structure is under a direct current, hence, there is an injection of electrons from a nCdS-layer in pSi and injection of holes from silicon in nCdS does not occur. As for ideal heterojunctions there is a parity of $M = (I_p/I_n) = \exp[-(E_{gn} - E_{gp})/kT]$,[25] where E_{gn}, E_{gp}–width of the band gaps of wide-band and narrow-band semiconductors, I_p, I_n-currents of holes and electrons, accordingly. The value of M shows that the current proceeds from the wide-band semiconductor to the narrow-band one. From parity for M follows that the more the difference between widths of the band gaps (ΔE_g) of these semiconductors is the more strictly the given parity is carried out. For example, at heterojunction between silicon and germanium, the parity between currents flowing from Si to Ge differs in e^{-16} times.[25] In our case the difference between width of band gaps of Si and CdS is 1.3 eV, whereas $\Delta E_g = 0.4$ eV for Si and Ge. From this it follows that the value of M for pSi–nCdS heterojunction should be much larger and the current in investigated structure is exclusively defined by electronic fluxes from nCdS into pSi. Above stated argument is true for an ideal heterojunction. In real heterojunctions, there are edge states on border of semiconductors and consequently the ratio M is not satisfied. The edge states are formed:

(a) because of more than 7% difference in crystal lattice constants of contacting pSi and nCdS[26] and
(b) by technological processes.

These edge states can be the centers of recombination or the tunneling centers for holes into the base of structure.

RESEARCH ARTICLE

Nevertheless, we believe that in structure the current is dominated by electronic fluxes going from In–nCdS-transition. Therefore the bend of zones occurs downwards. Besides, it is revealed that the value of surface potential changes strongly with growth of bias voltage value. For example, at giving of bias voltage $U = -1.12$ V on the top metal electrode the surface potential becomes equal to 0.48 eV. And at giving of positive bias voltage on the top metal electrode ψ_s from U changes rather poorly. For example, at giving of bias voltage $U = 27$ V ψ_s it is bent upwards on-0.24 eV. Such behavior of surface potential is caused by considerable density of edge states in the top half of silicon band gap. The experimental researches on distribution of edge states-N_{ss} from value of surface potential-ψ_{ss} confirm the above stated assumption (Fig. 5, curve 1). The curve of dependence N_{ss} (ψ_s) has the high density of edge states at positive values of surface potential and it becomes equal to $\sim 6 \cdot 10^{11}$ cm^{-2} at $\psi_s = -0.24$ eV. The value of N_{ss} in the bottom half of band gap is much less, than on top. For example, $N_{ss} \approx 9.5 \cdot 10^9$ cm^{-2} at $\psi_s = 0.08$ eV and $N_{ss} \approx 1.9 \cdot 10^{10}$ cm^{-2} at $\psi_s = 0.48$ eV.

From this it follows that the density of edge states in the bottom half of band gap has small values and they change little on power distance value $\sim$0.48 eV from the middle of the band gap. It should be noted that at the top as well as at the bottom half of the band gap, the certain density of edge states is effective and they have the charged conditions which do not include the values of neutral edge states like N_a^0-acceptor neutral edge states.

The above stated experimental results confirm that pSi–nCdS heterojunction with rather low density of edge states is received. At the same time it is known that the constant crystal lattices of cadmium sulfide and silicon differ by more than 7% and consequently between these semiconductors a heterojunction with low density of edge states should not be formed. Nevertheless, the experimental results reflected on Figure 6, curve 1 show that there is a relatively low density on border of pSi–nCdS heterojunction N_{ss}. These experimental results could be explained supposing formation of the heterojunction intermediate layer that smoothing a difference between lattice constants of cadmium sulfide and silicon. The solid solutions of pSi, nCdS or oxides SiO_x, CdO_x and SO_x can participate in such intermediate layers. However what intermediate layer is formed and what structure it has is not clear and that will be an object of the further research.

Now we consider capacitance–voltage characteristic after ultrasonic irradiation. As one can see from Figure 5, curve 2, the density of edge states in the bottom half of band gap of silicon after ultrasonic irradiation decreases slightly. For example, before ultrasonic irradiation $N_{ss} = 9.4 \cdot 10^9$ cm^{-2} at $\psi_{ss} = 0.02$ eV and at $\psi_{ss} = 0.48$ eV $N_{ss} = 1.9 \cdot 10^{10}$ cm^{-2}. After ultrasonic irradiation: $N_{ss} = 7.16 \cdot 10^9$ cm^{-2} at $\psi_{ss} = 0.02$ eV and at $\psi_{ss} = 0.48$ eV $N_{ss} = 1.4 \cdot 10^{10}$ cm^{-2}. This data shows that after ultrasonic irradiation the edge states in the bottom half of band gap are not enough annealed, they decrease by only $\sim$20%. The density of edge states at the top half of band gap also decreases after ultrasonic irradiation (Fig. 6, curve 2). The dynamics of change N_{ss} from value ψ_{ss} after irradiation (Fig. 5, curve 2) shows that the density of the edge states which are near the middle of the band gap are stronger annealed, than of being far from it. For example, before irradiation $N_{ss} = 5.07 \cdot 10^{10}$ cm^{-2} at $\psi_{ss} = 0.02$ eV and after ultrasonic irradiation $N_{ss} = 2.1 \cdot 10^{10}$ cm^{-2} at $\psi_{ss} = 0.02$ eV. At the same time $N_{ss} = 6 \cdot 10^{11}$ cm^{-2} at $\psi_{ss} = 0.24$ eV decreases to value $N_{ss} = 5 \cdot 10^{11}$ cm^{-2} after ultrasonic irradiation at the same value of surface potential. According to these experimental data, the edge states which are near to the middle of the band gap, decrease more than 2 times and N_{ss} located in the distance, exactly at $\psi_{ss} = 0.24$ eV, decrease just for 18% in the process of ultrasonic irradiation. Capacitance measurements done before and after ultrasonic irradiation confirm coherence of mechanisms of current flow in the structure with edge states of pSi–nCdS-heterojunction.

In a direct branch of CVC's current in dark and on light respectively, the spectral sensitivity increases by $\sim$20% after ultrasonic irradiation (Fig. 1 curve 1, 2), i.e., increases as much as the density N_{ss} in the bottom half of band gap of silicon on section border of pSi–nCdS heterojunction decreases. In inverse branch S_λ increases approximately twice (Fig. 1 curve 4, 5) that corresponds to reduction of value of edge states density in the top half of band gap of silicon which are responsible for recombinational processes. These results prove that at inclusion of pSi–nCdS–In-structure in a direct current direction, ("+"-potential on pSi) the electrons injection goes from the nCdS layer into the pSi-layer and recombinational processes are defined by edge states density which are in the bottom half of the band gap of silicon.

In the opposite current direction, there is an injection of electrons from pSi into nCdS layer and recombinational processes in structure and life time of electrons are defined by edge states in the top half of band gap. As N_{ss}, being near to the middle of the band gap, decreases approximately twice after USI, therefore the currents in the opposite direction and S_λ at bias voltage ($U \geq 8.5$ mV) also increase approximately twice. From this it follows that the density of edge states in pSi–nCdS heterojunction is a major factor influencing the spectral sensitivity of injection photo-detector based on pSi–nCdS–In-structure.

Till now we considered the current transfer, when bipolar drift and diffusive currents had small and about identical values. Thus, the bipolar drift current in high-resistance base (nCdS) was practically defined by minority equilibrium carriers (holes).

Now let us consider how an ultrasonic irradiation influences on current transfer of pSi–nCdS– In-structure at the big bias voltage both in direct and in the inverse current directions. The experiment shows that USI does not

RESEARCH ARTICLE

influence the regularity of a current flow in structure in direct and inverse branches of C–V characteristics in dark and on light and only increases the current values at the same value of bias voltage (Fig. 1). Illumination of structures was made by laser LG-75 with radiation power of 10–750 μW/cm^2 and with wavelength 0.625 μm and also from incandescent lamp with radiation of one lumen in visible spectrum at $9.1 \cdot 10^{-3}$ W.[15] In a direct branch of C–V characteristics both in dark and on light the current increases by $\sim$20% and in an inverse current branch it increases approximately twice (Fig. 1). In Tables I, II the values of spectral (S_λ) and integral (S_{int}) sensitivity are resulted at various white light intensities and at laser irradiation ($\lambda = 0.625$ μm) at various capacities and at different values of bias voltage before and after ultrasonic irradiation in direct and inverse current directions. As shown in Table I the values of S_{int} and S_λ in a direct current direction increase approximately by 20% after ultrasonic irradiation at all values of white light intensity and capacities of a laser irradiation and also bias voltage. The spectral and integral sensitivity of a photo-detector are increased more than 2 times in the opposite current direction after ultrasonic irradiation (Table II). Besides, according to Table II absolute values of S_{int} and S_λ are by four orders less, than their values in a direct current direction. At the same time the spectral sensitivity on value is more essential than S_λ of an ideal photo-detector. For example, at ideal photo-detector $S_\lambda = 0.5$ A/W[27] at $\lambda = 0.625$ μm. At this wavelength the spectral sensitivity in investigated structure is equal to 1.31 A/W at radiation power $P =$ 10 μW/cm^2 and $U = 5$ V and at greater values of bias voltage the value of S_λ became even higher (Table II). In an inverse branch of C–V characteristics relatively small values of S_{int} and S_λ are connected with occurrence of physical processes in base of structure and appearance of a sublinear section. In works[17,18] the physics of appearance of C–V characteristics' sublinear section which can be explained with existence of counter diffusive and drift currents in high-resistance base of structure is analyzed in details. Appearance of an extended sublinear section on inverse current–voltage characteristic of pSi–nCdS–In structure and value of dark and light currents on this site increase approximately twice after ultrasonic irradiation once again confirms that electrons are injected from pSi–nCdS-heterojunction into the high-resistance base (nCdS), which value, basically, is defined by property of pSi-nCdS heterojunction, exactly by density of border edge states. They also specify that ultrasonic irradiation does not influence the extent of a sublinear section and height of the Schottky potential barrier of In–nCdS which is an ideal transition in structure and minority non-equilibrium carriers of a hole are accumulated near it and diffusive currents directed towards to drift and diffusive currents, ongoing from pSi–nCdS-heterojunction are created. Thus, it is necessary to notice that the height of the Schottky potential barrier for minority non-equilibrium carriers (holes) increases with growth of inverse bias voltage value which does not change after ultrasonic irradiation.

From this data also follows, that those non-equilibrium plasmas of electron–hole pairs do not relax in structure base at the expense of recombination and on border of the barrier In–nCdS. For the proof of the given statement the value of life time of minority carriers (holes) from inverse current–voltage characteristics has been estimated.

The carried out analysis shows that in a range of current density $I \approx (1.3 \cdot 10^{-8}$–$2.2 \cdot 10^{-7})$ A/cm^2 C–V characteristic is described by exponential dependence of type $I = I_{01}\exp$ (qU/c kT), at which exponent index $c = 8.2$ and pre-exponential multiplier $I_{01} = 1.8 \cdot 10^{-8}$ A/cm^2.

From the literature it is known that if accumulation effect is not essential, from C–V characteristics variety in diffusive mode remain only well-known dependences $I \sim \exp$ (qU/kT) and $I \sim \exp$ (qU/c kT), for the first time obtained by Shokli[28] and Stafeev[29] for p–n-diode structures with ohmic contact and with considerable resistance of base.

According to the theory,[19] in structures with considerable resistance of base, a diffusion current flows and it is described by following analytical expression:

$$I = I_{01} \exp(\text{qU}/\text{c kT}) \tag{2}$$

where $$c = (2b + c h\text{w}/\text{L} + 1)/(b+1) \tag{3}$$

Table I. Dependence of integral (S_{int}), spectral (S_λ) sensitivities of light exposure (E_{lux}), laser irradiation power (P) and bias voltage (U) before and after ultrasonic irradiation at direct bias voltage.

White light				At laser irradiation		
Lightening		Before USI	After USI	Capacity	Before USI	After USI
E(lux)	U(V)	S_λ, (A/W)	S_λ, (A/W)	P(μ W/cm^2)	S_λ, (A/W)	S_λ, (A/W)
0.05	5	$0.26 \cdot 10^4$	$0.316 \cdot 10^4$		36	42.85
	10	$4.2 \cdot 10^4$	$5 \cdot 10^4$	0.7	550	660
	20	$4.47 \cdot 10^4$	$5.4 \cdot 10^6$		50358	60428
1	5	$0.2 \cdot 10^3$	$0.23 \cdot 10^3$	50	7.4	8.86
	10	$3.32 \cdot 10^3$	$3.98 \cdot 10^3$		121.5	145.8
	20	$3.4 \cdot 10^5$	$4.1 \cdot 10^5$		8236	9992

Table II. Dependence of integral (S_{int}), spectral (S_λ) sensitivities of light exposure (E_{lux}), laser irradiation power (P) and bias voltage (U) before and after ultrasonic irradiation at direct bias voltage.

White light				At laser irradiation		
Lightening		Before USI	After USI	Capacity	Before USI	After USI
E(lux)	U(V)	S_λ, (A/W)	S_λ, (A/W)	P(μW/cm^2)	S_λ, (A/W)	S_λ, (A/W)
0.1	5	40.1	80.2	10	1.31	2.62
	10	47.36	94.72	10	1.883	3.766
	60	76	152		3.28	6.56

here: $b = \mu_n/\mu_p$-electrons and holes mobility ratio, a w-base thickness, c-exponent index, I_0-pre-exponential multiplier, q-electron charge, k-Boltzmann constant, T-temperature in Kelvin degrees, V-bias voltage. The quantities "c" and "I_0" have rather small values for C–V characteristics section to a site value. Substituting experimental value $c = 8.2$, obtained from C–V characteristics, to the Eq. (3), we find that diffusive length of holes $L_p = 0.45$ μm, $\mu_p\tau_p = 7.8 \cdot 10^{-8}$ cm^2/V (product of mobility for holes life period) at values: $b = 38$,[14] $w = 2$ μm, $\mu_n = 285$ cm^2/V $\cdot$ s and $\mu_p = 7 \div 8$ cm^2/V $\cdot$ s.

Further, using expressions for $\mu_p\tau_p = 7.8 \cdot 10^{-8}$ cm^2/V and value for holes mobility $\mu_p = 7 \div 8$ cm^2/V $\cdot$ s and base thickness $w = 2$ μm we find that $\tau_p \approx 10^{-8}$ cm^2/V. We estimate flight time of non-equilibrium minority carriers through base from a sub-linear C–V characteristics section which has appeared to be equal $\sim 5 \cdot 10^{-10}$ s–$8 \cdot 10^{-11}$ s correspondingly at the beginning and at the end of the given site at values $w = 2$ μm and $\mu_p = 7 \div 8$ cm^2/V $\cdot$ s. From this it follows that non-equilibrium carriers reach the anode without lost. In this case the anode role plays barrier In–nCdS where probably are to be expected losses of non-equilibrium minority carriers. It is known[26] that semiconductor materials with considerable ionic conductivity at barrier on their basis form little edge states, therefore the loss of non-equilibrium carriers of a charge here is not considerable either. The resulted estimations confirm that the quantity of injected electrons is defined by property of pSi–nCdS-heterojunction.

The sublinear C–V characteristics section is also observed on a straight line of current voltage characteristic (Fig. 1). From Figure 1 it is clear that the sublinear section in a direct branch of C–V characteristics is observed in a range of voltage $U = 1$–5 V where the current is 130–160 μA/cm^2 that is, on two orders more and its interval is much less, than in the opposite current direction. The sublinear section in a direct C–V characteristics branch is notable for that its ahead and back have exponential current behavior sites on voltage, like

$$I = I_0[\exp(qU/c\ kT) - 1] \tag{4}$$

where "c" and "I_0" quantities are considerably different. It means that on C–V characteristics section going after a sub-linear C–V characteristics section the charging conditions of strongly compensated recombination centers change, in a result of which the lifetime of minority charge carriers in (nCdS) base decreases and regularity of current flow changes. The carried out analysis of C–V characteristics sites before and after a sub-linear site confirms an above stated thoughts. On exponential site a current from voltage to a sub-linear site has exponent index $c_1 = 3.6$, $I_{02} = 5.4 \cdot 10^{-9}$ A/cm^2. Substituting experimental value of $c_1 = 3.6$ in the Eq. (3) we find that: $L_p = 0.48$ μm, $\mu_p\tau_p = 8.8 \cdot 10^{-8}$ cm^2/V and $\tau_p \approx 10^{-8}$ s at values $b = 38$, $\mu_p \approx 8$ cm^2/V $\cdot$ s, $w = 2$ μm. As quantity I_{01} is approximately equal to a current at which conductivity of base area increases twice by injection, i.e., equilibrium and non-equilibrium conductivity of thickness are compared and there comes transition to high levels of injection. Therefore supposing that $I_0 = 5.4 \cdot 10^{-9}$ A/cm^2 there corresponds to initial voltage of the second C–V characteristics section (0.1 V) we find that specific resistance of base $\rho = 1.5 \cdot 10^{10}$ $\Omega \cdot$ cm.

The C–V characteristics section after a sub-linear site is described by exponential dependence $I = I_{03}\exp(\mathrm{qU}/c_2\ \mathrm{kT})$, where $c_2 = 68$, $I_{03} = 1.9 \cdot 10^{-7}$ A/cm^2. Substituting these experimental data to the Eqs. (3) and (4) we define that the relation of a base thickness to length of holes diffusion is: w/L$_p = 8.5$, $L_p \approx 0.24$ μm, $\mu_p\tau_p \approx 2.2 \cdot 10^{-8}$ s, $\tau_p \approx 2.8 \cdot 10^{-9}$ s and specific resistance of base $\rho = 1.9 \cdot 10^7$ $\Omega \cdot$ cm. The quantities L_p, τ_p and ρ estimated of this C–V characteristics section strongly differ for the same quantities calculated from a site to be before a sub-linear site. Distinction between these quantities is explained by change of base properties with growth of current density in a structure. The spent estimations confirm completely that the base of investigated diode structure after a sublinear C–V characteristics section changes its property because of a recharge of strongly compensated recombination centers in which result the life time of minority carriers (holes) decreases and a structure has a property of "long" diodes[30] in which the current is defined basically by the drift mechanism.

Presence of an extended sub-linear site in the opposite current direction means that the barrier of nCdS–In is more perfect, than at pSi–nCdS-heterojunction and a height of the potential barrier for non-equilibrium minority carriers of holes is more than at heterojunction. Therefore

RESEARCH ARTICLE

non-equilibrium holes are accumulated near pSi–nCdS-heterojunction rather at small voltage values and at the big voltage they pass to pSi-layer.

5. CONCLUSION

It is shown that in spectral distribution of a photocurrent the sign inversion point is observed when towards directed bipolar drift current is completely compensated by bipolar diffusive current. Shift of inversion point of photosensitivity sign towards the short wavelengths is defined by magnitude of bipolar diffusive current which appears because of electrons injection in base from pSi–nCdS heterojunction of a photo voltage and giving of inverse bias voltage. It is established that a direct current in pSi–nCdS–In-structure is limited by recombination processes for which edge states (N_{ss}) in the bottom half of band gap are responsible and inverse currents are defined by N_{ss} being in the top half of band gap of silicon on section border of pSi–nCdS heterojunction.

The capacitance–voltage method reveals distribution of edge states density depending on surface potential on pSi–nCdS-hetero-border. Thus, it is shown that dependence of N_{SS} from ψ_S has a complex character. In the bottom half of band gap N_{ss} changes from $\approx 9.4 \cdot 10^9$ cm^{-2} to $1.9 \cdot 10^{10}$ cm^{-2} on energy distance 0.48 eV from center of the band gap and in the top half the density of edge states changes from $\approx 5.7 \cdot 10^{10}$ cm^{-2} to $6 \cdot 10^{11}$ cm^{-2}, at change of ψ_S from 0.02 eV to 0.24 eV. The results obtained allow to assert that pSi–nCdS-heterojunction has a low enough density of edge states, that has allowed to receive an injection photo-detector based on pSi–nCdS–In-structure with high spectral ($S_\lambda = 5.04 \cdot 10^4$ A/W) and integral ($S_{\text{int}} = 2.8 \cdot 10^4$ A/lm or $4.47 \cdot 10^6$ A/W) sensitivity in a direct current direction. It is established that the ultrasonic irradiation power of 1 W and frequency of $f = 2.5$ MHz during 15 min leads to reduction of edge states density on pSi–nCdS-hetero-border. Dependence N_{SS} from ψ_S has different regularity in bottom and in the top half of width of the band gap after USI irradiations. In the bottom half density of edge states decreases approximately by 20% and its distribution from surface potential has a constant character. In the top half N_{SS} decreases 2 times near the center of the band gap and at big values of $\psi_S \approx 0.24$ eVB it decreases just by 20%. From this it follows that dependence of N_{SS} (ψ_S) after ultrasonic irradiation has a complex character.

It is revealed that increase in values of direct and inverse CVC's currents and also increase of value of integral (S_{int}) and spectral (S_λ) sensitivity of injection photo-detector based on pSi–nCdS–In-structure is caused by reduction of edge states density on the pSi–nCdS heterojunction interface.

References and Notes

1. I. M. Koldaev, V. V. Losev, and B. M. Orlov, *PhTC* 18, 1316 **(1984)**.
2. Sh. A. Mirsagatov and A. K. Uteniyazov, *TPhJ Letters* 38, R.1, 70 **(2012)**.
3. S. A. Mirsagatov, R. R. Kabulov, and M. A. Makhmudov, *PhTC* 47, 815 **(2013)**.
4. Sh. A. Mirsagatov, O. K. Ataboev, and B. N. Zaveryukhin, *PhTC* 11, 4 **(2013)**.
5. A. S. Saidov, A. Yu. Leyderman, Sh. N. Usmonov, and K. T. Kholikov, *PhTC* 43, R.4, 436 **(2009)**.
6. P. I. Baransky, A. E. Belyaev, S. M. Koshirenko, et al., *PhSB.* 32, 2159 **(1990)**.
7. I. V. Ostrovskiy, L. P. Stoblenko, and A. B. Nadtochiy, *PhTC.* 34, 257 **(2000)**.
8. E. B. Zaveryukhina, N. N. Zaveryukhina, L. N. Lezilova, B. N. Zaveryukhin, etc. *TPhJ Letters* 31, 54 **(2005)**.
9. O. Ya. Olikh, *PhTC* 45, 816 **(2011)**.
10. A. Davletova and S. Zh. Karazhanov, *J. Phys. D: Appl. Phys.* 41, 165 **(2008)**.
11. I. G. Pashaev, *PhTC* 46, 1108 **(2012)**.
12. I. B. Sapaev, *SAS. Uzbekistan* 2, 27 **(2013)**.
13. E. Frisch, Optical methods of measurements. Part I. Ed. of Leningrad University **(1976)**.
14. V. I. Fistul, Physics and chemistry of a solid body. (M, Metallurgy) t. I II. **(1995)**.
15. http://zaz.gendocs.ru/docs/2800/index-1621226.html.
16. A. M. Lampert and P. Mark, Current Injection in Solids, Academic Press New York and London **(1970)**.
17. E. I. Adirovich, P. M. Karageorgiy-Alkalaev, and A. Yu. Leyderman, *Current of double injection in semiconductors. (M, "The Soviet radio")* **(1978)**.
18. P. M. Karageorgiy-Alkalaev and A. Yu. Leyderman, *Tashkent, Ed. "FAN", Uzbek Soviet Socialist Republic* **(1981)**.
19. V. I. Stafeev and V. M. Tuchkevich, Rep. 19th Ann. Conf. Phys. Electr. MIT, Cambridge, Massach **(1959)**.
20. I. D. Anisimova, I. M. Vikulin, F. A. Zaitov, and Sh. D. Kurmashev, *Under. Red. Stafeev* 1, 101 **(1984)**.
21. I. M. Vikulin, S. D. Kurmashev, and V. I. Stafeev, *PhTC.* 42, R.1, 113 **(2008)**.
22. S. M. Sze, Physics of Semiconductor Devices, A Wiley–Interscience Publication John Wiley and Sons New York, Chichester, Brisbane, Toronto, Singapore **(1981)**, V. 1.386.
23. V. G. Georrgiu, Capacity–voltage measurements of semiconductors parameters (Kishenev "Shtiintsa") **(1987)**.
24. S. A. Mirsagatov and A. K. Uteniyazov, *TPhJ Letters* 38, R. 1, 70 **(2012)**.
25. I. M. Vikulin and V. I. Stafeev, Physics of Semi-Conductor Devices, Moscow "The Soviet radio" **(1980)**.
26. A. Milns and D. Foykht, Heterojunctions and transitions of metal-semiconductor. Under the editorship of professor V. S. Vavilov, Publishing house "Mir." Moscow **(1975)**.
27. A. Ambrozyak, Construction and Technology of Semi-Conductor Photoelectric Devices, Moscow, Ed. "The Soviet radio" **(1970)**.
28. Shockley, *Bell Syst. Techn. J* 28, 4351 **(1949)**.
29. V. I. Stafeev, *TPhJ* 28, 1631 **(1958)**.
30. B. Osipov and V. I. Stafeev, *PhTC* 1, R.12, 1796 **(1967)**.

Received: 25 February 2014. Accepted: 20 May 2014.

RESEARCH ARTICLE